Applied Catalysis B: Environmental 92 (2009) 429–436

Contents lists available at ScienceDirect

Applied Catalysis B: Environmental

journal homepage: www.elsevier.com/locate/apcatb

Properties and performance of Pd based catalysts for catalytic oxidation of volatile organic compounds

Sang Chai Kim [a,*], Wang Geun Shim [b]

[a] Department of Environmental Education, Mokpo National University, 61 Dorim-ri, Cheonggye-myeon, Muan 534-729, Republic of Korea
[b] Faculty of Applied Chemical Engineering, Chonnam National University 300, Yongbong-dong, Buk-gu, Gwangju 500-757, Republic of Korea

ARTICLE INFO

Article history:
Received 5 June 2009
Received in revised form 11 August 2009
Accepted 1 September 2009
Available online 4 September 2009

Keywords:
Pd based catalyst
Oxidation state
Growth of Pd particle
Volatile organic compound
Catalytic oxidation

ABSTRACT

Catalytic oxidations of volatile organic compounds (VOCs) (benzene, toluene and *o*-xylene) over 1 wt% Pd/γ-Al_2O_3 catalyst were carried out to assess the properties and performance of the Pd based catalyst. The properties of the prepared catalysts were characterized by the Brunauer Emmett Teller (BET) surface area, H_2 chemisorption, X-ray photoelectron spectroscopy (XPS), X-ray diffraction (XRD), and transmission electron microscopy (TEM) analyses. The experimental results revealed a significant increase in VOCs conversion with the lapse of the reaction time at certain reaction temperatures. On the other hand, the hydrogen pretreated 1 wt% Pd/γ-Al_2O_3 catalyst, whose shape of conversion curve is similar to the non pretreated catalyst, led the conversion curves for the total oxidation of VOCs to be shifted to lower temperature. It was also found that such increases in VOCs conversion were highly dependent on the oxidation state of Pd and the growth of Pd particles in the catalyst. In addition, in the case of the catalyst consisting of the same oxidation state (PdO/Pd^{2+} or Pd^0), the particle sizes possibly play a more important role in the catalytic activity. The activity order of 1 wt% Pd/γ-Al_2O_3 catalyst with respect to the VOC molecule was *o*-xylene > toluene > benzene.

1. Introduction

The drastically increasing environmental consciousness in the last two decades has roused people to reducing volatile organic compounds (VOCs) because of their harmful effects on human health and the environment. Among the many technologies available to control VOCs such as oxidation, adsorption and absorption, the complete oxidation of these pollutants to carbon dioxide and water has been identified as the most efficient way to destroy VOCs. Especially, the catalytic oxidation has attracted much attention because of low thermal NO_x emissions, highly destructive efficiency, low energy cost, and a relatively high flexibility compared to the thermal oxidation [1–4]. However, the high temperature catalytic oxidation process for the removal of low concentrations of VOCs requires higher operating cost because of the higher energy requirement. Therefore, highly active catalysts which work at lower temperatures are required [5].

Currently, various kinds of catalysts such as supported noble metals and supported transition metals are being extensively used for complete oxidation of VOCs [6–13]. As to the activity, selectivity and stability of the catalysts for catalytic oxidation, the supported noble metals have been generally regarded as the most desirable catalysts. In particular, the palladium (Pd) based catalysts offer several advantages such as high activity, thermal stability, good performance as well as low cost compared to the platinum (Pt) based catalysts [6–8,14–17].

Although the phenomena, which influence the catalytic oxidation over the palladium based catalysts, has been investigated by several researchers, the effect of the oxidation state and the particle size of Pd on the catalytic hydrocarbon oxidation still remains controversial. Many researchers have suggested that the performance of Pd supported catalysts for the oxidation of VOCs is highly dependent on the oxidation state of Pd. Some authors suggest that metallic species (Pd^0) are more active than the oxide form (PdO/Pd^{2+}) for catalytic oxidation [18–23] while the others affirm just the opposite [19,20]. As for the effect of Pd particle size, some works have shown a correlation between the particle size and the catalytic activity [24–26]. On the other hand, several authors have not observed a strong dependence between the particle size and the catalytic activity [27–29]. In addition, Farrauto et al. [30], and Lyubovsky and Pfefferle [31] have reported that the oxidation state of the catalyst, metal–support interactions, and catalyst particle morphology are interdependent parameters, which strongly influence the activity of the catalyst during the reactor cooling cycle. Also, Ferreira et al. [15] and Demoulin et al. [32] have reported that the variations of catalytic activities are closely related to the particle size and support, although the effect of the size on the catalytic reaction is still arguable. Recently, Baylet

* Corresponding author. Tel.: +82 61 450 2781; fax: +82 61 450 2780.
E-mail address: gikim@mokpo.ac.kr (S.C. Kim).

0926-3373/$ – see front matter
doi:10.1016/j.apcatb.2009.09.001

et al. [33] have observed that the supported palladium catalyst with higher palladium dispersion (i.e. smaller crystal size), shows higher catalytic activity for the methane oxidation reaction.

In this work, we studied the influence of the changes in the Pd particles in Pd based catalyst on the VOCs conversion during the reaction. VOCs such as benzene, toluene and *o*-xylene (BTX) were chosen as model compounds for their toxic, carcinogenic and different molecular properties. The changes in the physicochemical state of the catalysts were examined by using BET surface area, H_2 chemisorption, XPS, XRD and TEM analyses.

2. Experimental

2.1. Catalyst preparation and characterization

The conventional incipient wetness impregnation method was followed to prepare Pd/γ-Al_2O_3 catalyst from a mixture of palladium chloride solution (Aldrich Co., Ltd.) and powdered γ-Al_2O_3 (Asian Catalyst Co., Ltd.) The impregnated samples were dried at 120 °C in an oven for overnight. Then the dried samples were calcined at 400 °C for 6 h in a furnace to obtain the final form of supported catalysts. The prepared catalyst contained 1 wt% Pd. In addition, the hydrogen pretreated catalyst was prepared by treating 1 wt% Pd/γ-Al_2O_3 catalyst with hydrogen at 300 °C for 2 h. The Brunauer Emmett Teller (BET) surface areas of all samples were determined by nitrogen adsorption data obtained at −196 °C (Micromeritics ASAP 2020 analyzer). Prior to nitrogen sorption analysis, all the samples were degassed under vacuum (5×10^{-3} mmHg) for 6 h at 250 °C. The crystal structures of samples used in this work were examined by X-ray diffraction (XRD) using a Phillips PW3123 diffractometer equipped with a graphite monochromator and Cu Kα radiation of wavelength 0.154 nm. Here, the samples used were investigated in the 2θ range of 20–90° at a scanning speed of 70°/h. An X-ray photoelectron spectroscopy (XPS) analysis was conducted using a photoelectron spectrometer VG Scientific MultiLab 2000 system equipped with a non-monochromatic Mg Kα radiation of 1253.6 eV. The C 1s peak (285.0 eV) obtained from XPS analysis was used to calibrate the binding energy values. The images of transmission electron microscope (TEM) were obtained using a JEOL JEM-2000FAXII at an acceleration voltage of 200 kV. To investigate the surface area and dispersion of palladium, hydrogen chemisorption measurements (Quantachrome, ChemBet 3000) were performed using the excess pulse technique. 0.4 g of catalyst sample was first purged by a N_2 flow (50 cc min^{-1}) to remove moisture and then reduced by a N_2 flow containing 5 vol.% H_2 (50 cc min^{-1}) at 400 °C for 1 h. Residual H_2 was removed by a N_2 flow (50 cc min^{-1}) at 400 °C for 1 h, and chemisorption uptake was then measured at room temperature. A pulse of H_2 of known volume was injected into a He carrier stream, and the amount of H_2 chemisorbed by the sample was determined from the difference in thermal conductivity detector (TCD) response before and after passage across the detector.

2.2. Catalytic oxidation

The purity and manufacturer of each BTX are as follows: benzene, 99.5% (Fisher Chemical Co.); toluene, 99.5% (Fisher Chemical Co.) and *o*-xylene, 95.0% (Fisher Chemical Co.). All chemicals were used as received without any further treatment. The complete oxidations of BTX were carried out using a conventional fixed bed flow reactor as reported in our previous work [10]. The reactor has three major sections, namely (i) apparatus for preparation of vapors, (ii) fixed bed flow reactor in a heating system, and (iii) apparatus for the analysis of reactants and products. The catalytic reactor (quartz tube with "I" shape) consisted of a vertical tubular of 1.0 cm diameter and 35 cm length in an electrical heating system controlled by a proportional integral derivative (PID) controller. In each run, 0.2 g of catalyst was loaded in the middle of the reactor supported by quartz wool. For accurate and stable controlling of the gas flow rates, the mass flow controllers (UNIT Instrument, UFC-8100) were used. The concentration of each component was 1000 ppm, which was controlled by the temperature of the saturator and the additional air stream. The flow rate of the gas mixture through the reactor was 100 cm^3 min^{-1}, which gave a gas hourly space velocity (GHSV) of 15,000 h^{-1}. All the lines were heated sufficiently at 120 °C to prevent the adsorption and condensation of the reactant and the product in the tubes. The concentration of inlet and exit gas stream was determined using a gas chromatograph (Shimadzu, GC-14A) equipped with thermal conductivity. The chromatographic columns used were composed of a 5% bentone-34 and 5% dinonyl phthalate/shimalite (60–80 mesh, Φ 3 mm × 3 m) for BTX analysis, MS 5A for CO separation and a Porapak Q (50–80 mesh, Φ 3 mm × 3 m) for CO_2 separation. The GC/MS (Shimadzu, QP5050) was also employed for the quantitative and qualitative analysis of the products and by-products. The conversion was calculated on the basis of hydrocarbon consumption.

3. Results and discussion

Blank tests for benzene, toluene and *o*-xylene were conducted without a catalyst to examine the effect of quartz wool and the quartz reactor. No activities (homogeneous reaction) were observed below 400 °C. These results indicate that the employed system may be applied for analyzing the catalytic oxidation of VOCs.

3.1. BTX oxidation over 1 wt% Pd/γ-Al_2O_3 catalyst

The experimental results of BTX over 1 wt% Pd/γ-Al_2O_3 catalyst (conversion of benzene, toluene or *o*-xylene with time on stream at certain reaction temperature) are shown in Figs. 1–3, respectively. The only product in the experiments was CO_2, and no CO was detected at any point during this experimental run. As shown in Fig. 1, the reaction began to take place at the reaction temperature of at 240 °C, where the benzene conversion was 2.1% and slowly increased with increasing reaction temperature of up to 260 °C. There was no significant increase in conversion with the lapse of

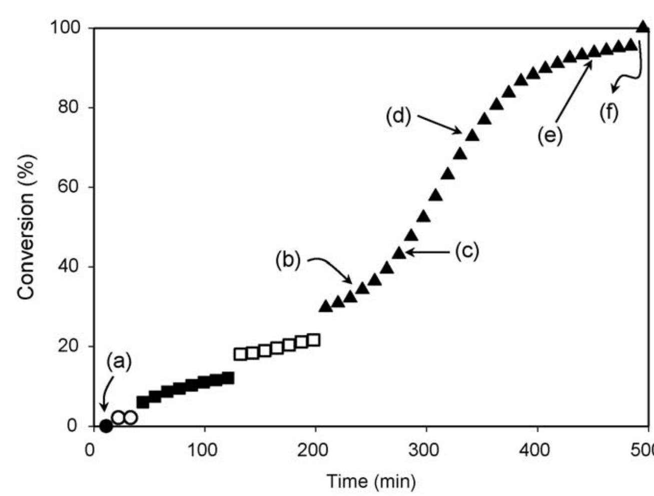

Fig. 1. Benzene conversion with time on stream over 1 wt% Pd/γ-Al_2O_3 catalyst. Reaction condition: catalyst weight = 0.2 g; toluene concentration = 1000 ppm; total flow rate = 100 cc min^{-1}. (●) 230 °C, (○) 240 °C, (■) 250 °C, (□) 260 °C, (▲) 270 °C.

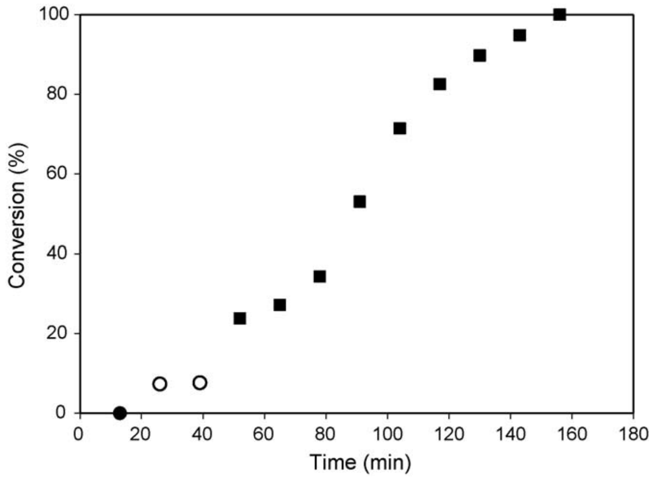

Fig. 2. Toluene conversion with time on stream over 1 wt% Pd/γ-Al_2O_3 catalyst. Reaction condition: catalyst weight = 0.2 g; toluene concentration = 1000 ppm; total flow rate = 100 cc min^{-1}. (●) 200 °C, (○) 210 °C, (■) 220 °C.

Table 1
Basic properties of 1 wt% Pd/γ-Al_2O_3 catalyst.

Catalyst	BET surface area ($m^2\,g^{-1}$)	Metal surface area ($m^2\,g^{-1}$)	Dispersion (%)
Fresh catalyst	151.0	2.82	63.3
Catalyst used in this experiment[a]	149.1	1.16	26.1
Used catalyst	148.2	0.82	18.4

[a] Catalyst after 230 min on stream at 270 °C in Fig. 1(e).

the reaction time at each reaction temperature (240, 250 and 260 °C). However, the benzene conversion gradually increased from 29.8% to 100% after running for approximately 300 min on stream at the reaction temperature of 270 °C. The arrows in Fig. 1 show the points when the sample was collected from the reactor for the XPS and the TEM analyses.

Figs. 2 and 3 show the conversion of the toluene and the *o*-xylene oxidations with time on stream over 1 wt% Pd/γ-Al_2O_3. The toluene and the *o*-xylene oxidations began to take place at the reaction temperatures of 210 and 200 °C, respectively, where each conversion was 7.3% and 7.5%, respectively. Here, the toluene conversion hardly changed with the lapse of the reaction time at

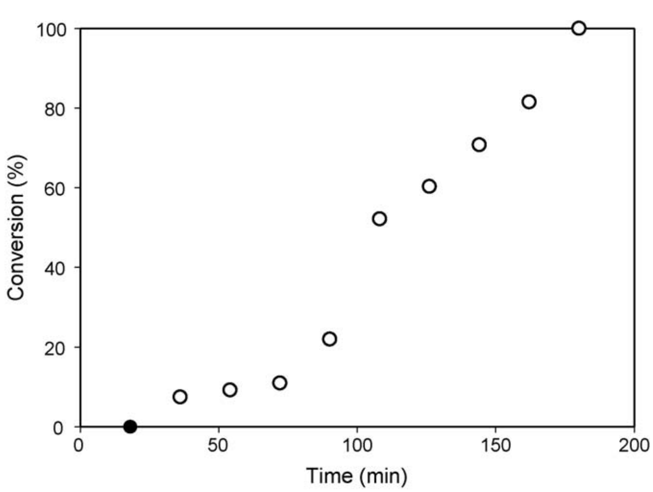

Fig. 3. Xylene conversion with time on stream over 1 wt% Pd/γ-Al_2O_3 catalyst. Reaction condition: catalyst weight = 0.2 g; toluene concentration = 1000 ppm; total flow rate = 100 cc min^{-1}. (●) 190 °C, (○) 200 °C.

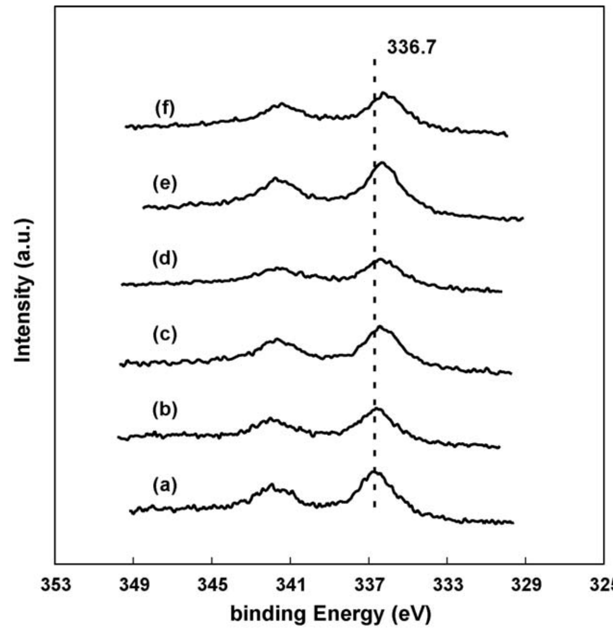

Fig. 4. XPS spectra of 1 wt% Pd/γ-Al_2O_3 catalyst: (a) the fresh catalyst, (b) the catalyst after 30 min on stream at 270 °C in Fig. 1, (c) the catalyst after 80 min on stream at 270 °C Fig. (d) the catalyst after 140 min on stream at 270 °C in Fig. 1, (e) the catalyst after 230 min on stream at 270 °C in Fig. 1, (f) the used catalyst in Fig. 1.

the reaction temperature of 210 °C. However, the gradual increases in the toluene and the *o*-xylene conversions were noted from 29.8% to 100% and from 7.5% to 100% after running for approximately 140 and 160 min on stream at the reaction temperatures of 220 and 200 °C, respectively.

Subsequently, it was observed that all three VOCs conversions increased with the lapse of the reaction time at certain reaction temperatures (at 270 °C for benzene, at 220 °C for toluene and at 200 °C for *o*-xylene). In addition, the comparison of benzene, toluene and *o*-xylene conversions on the basis of reaction temperature reveals that this activity sequence of 1 wt% Pd/γ-Al_2O_3 catalyst with respect to the VOC molecule is *o*-xyle-

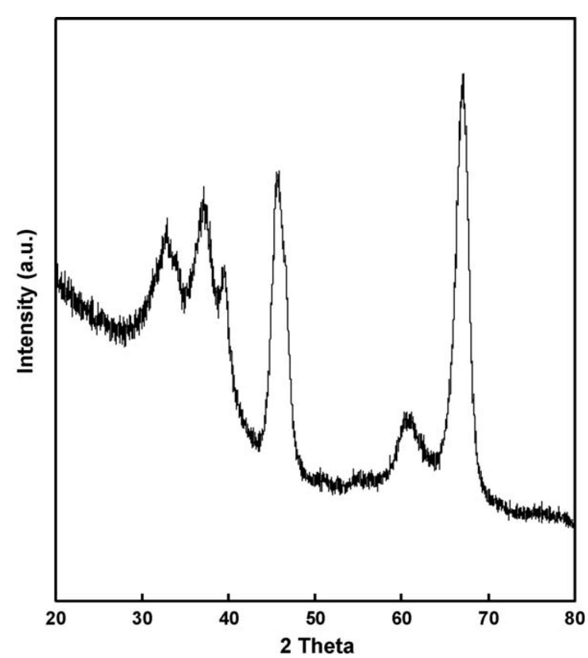

Fig. 5. XRD patterns of 1 wt% Pd/γ-Al_2O_3 catalyst.

ne > toluene > benzene. This result indicates that the activity sequence is consistent with the values of the ionization potentials of the methyl derivatives (9.24 eV for benzene, 8.82 eV for toluene and 8.56 eV for *o*-xylene). Therefore, benzene is the most difficult to oxidize.

Basic properties of the fresh catalyst, the catalyst used in this experiment (the arrow (d) in Fig. 1) and the used catalysts (the arrow (f) in Fig. 1), such as BET surface areas, metal surface area and metal dispersion are summarized in Table 1. Their BET surface areas were similar within the experimental error, as shown in Table 1. On the other hand, the metal surface area and its dispersion decreased considerably with the lapse of the reaction time.

The XPS analysis, which usually provides highly useful information about the physicochemical characteristics of the heterogeneous catalysts, was conducted to investigative the oxidation state of the fresh catalyst, the catalysts used in this experiment and the used catalyst. The Pd $3d_{5/2}$ XPS peaks and the binding energy values of the fresh catalyst (the arrow (a) in Fig. 1), the catalyst used in this experiment (the arrows (b)–(e) in Fig. 1) and the used catalyst (the arrow (f) in Fig. 1) are shown in Fig. 4. The binding energies (BE) of Pd $3d_{5/2}$ for six samples are 336.7, 336.4, 336.3, 336.3, 336.2 and 336.2 eV, respectively. Though the core level BE of palladium (Pd $3d_{5/2}$) slightly decrease, the BE values of all the catalysts fall under the category of those of the characteristics of oxidized state (PdO/Pd^{2+}) [15]. Accordingly, since the oxidation state changes on the catalyst surface were not observed at these samples, it seems that the oxidation state of the catalyst surface is not associated with the increase of the VOCs conversions with the lapse of the reaction time at certain reaction temperatures (at 270 °C for benzene, at 220 °C for toluene and at 200 °C for *o*-xylene) in Figs. 1–3. The XRD patterns of 1 wt% Pd/γ-

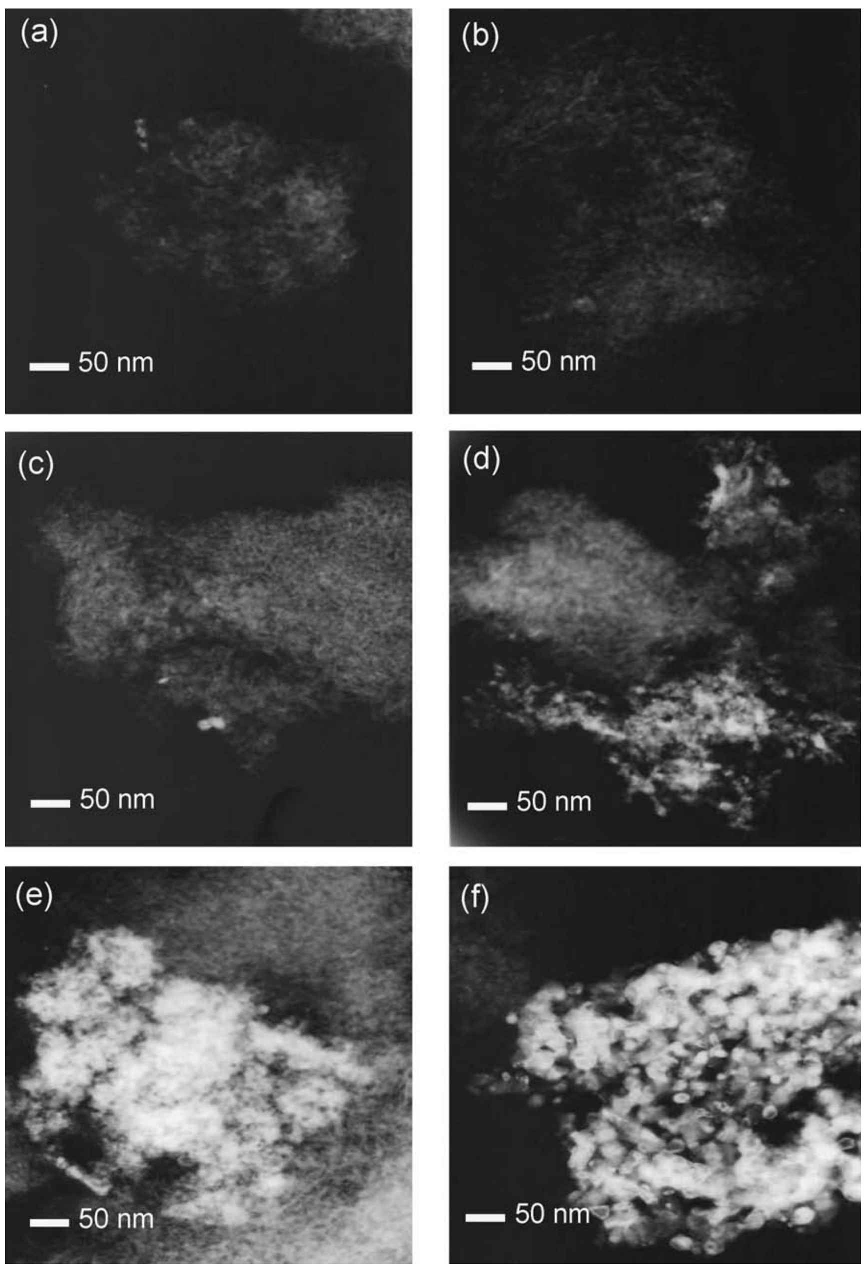

Fig. 6. TEM photographs of 1 wt% Pd/γ-Al_2O_3 catalyst: (a) the fresh catalyst, (b) the catalyst after 30 min on stream at 270 °C in Fig. 1, (c) the catalyst after 80 min on stream at 270 °C in Fig. (d) the catalyst after 140 min on stream at 270 °C in Fig. 1, (e) the catalyst after 230 min on stream at 270 °C in Fig. 1, (f) the used catalyst in Fig. 1.

Al_2O_3 catalyst are shown in Fig. 5. As can be seen in this figure, the only peaks observed are γ-Al_2O_3 diffraction peaks. This information clearly indicates the well dispersed Pd species on the support.

The TEM images of the fresh catalyst, the catalysts used in this experiment, and the used catalyst are shown in Fig. 6. These results of TEM analyses were used to investigate the changes in Pd particle size and morphology of 1 wt% Pd/γ-Al_2O_3 catalyst. The TEM image of the fresh sample is shown in Fig. 6(a). The Pd particles, showed as whiter spots, seem to be well dispersed and have a homogeneous size between 7 and 10 nm. The TEM images obtained after the reaction in benzene oxidation are shown in Fig. 6(b)–(f) (the same as the arrows (b)–(f) in Fig. 1). Fig. 6(b) represents the TEM image of the catalyst, which was collected after 30 min on stream at 270 °C. At this point the particle sizes insignificantly changed compared to those of the fresh catalyst. The TEM images of the catalyst samples, which were collected after 80, 140 and 230 min oxidation on stream and the used catalyst (Fig. 6(c)–(f)) at an equal temperature showed that Pd particle sizes gradually increased with the lapse of the reaction time to approximately 18–36 nm. Most of the particles appeared to be lacking any pronounced faceting. In addition, as shown in Table 1, the decreases of metal surface area and Pd dispersion can be attributed to the growth of Pd particles. Accordingly, it appeared that increasing the lapse of the reaction time at certain temperatures (at 270 °C for benzene, at 220 °C for toluene and at 200 °C for *o*-xylene) resulted in increasing the Pd particle size of the catalyst, subsequently, improving the catalytic activity. Therefore, these results led us to conclude that the increase in the VOC conversions is highly dependent on the growth of Pd particles.

3.2. BTX oxidation over 1 wt% Pd/γ-Al_2O_3 catalyst pretreated with hydrogen

Figs. 7–9 show the conversion of the benzene, toluene and *o*-xylene oxidations with time on stream over 1 wt% Pd/γ-Al_2O_3 catalyst pretreated with hydrogen. The pattern of VOCs conversion over 1 wt% Pd/γ-Al_2O_3 catalyst pretreated with hydrogen was similar to that of VOCs conversion over 1 wt% Pd/γ-Al_2O_3 catalyst. However, the hydrogen pretreatment led the conversion curves for the total oxidation of VOCs to be shifted to lower temperature. For instance, as shown in Fig. 7, the benzene oxidation began to take place at the reaction temperature of 200 °C, where the benzene conversion was 4.0%, and the benzene conversion slowly increased with increasing reaction temperature and gradually increased from 26.3% to 91.2% after running for approximately 340 min on stream at the reaction temperature of 240 °C and reached the complete oxidation (100%) at the reaction temperature of 250 °C. In addition, the shapes of conversion curves of toluene and *o*-xylene oxidation were similar to that of the benzene oxidation. Accordingly, the hydrogen pretreated catalyst resulted in lowering the reaction temperatures for the initiation and completion of oxidations of benzene, toluene and *o*-xylene by 40, 60, 60, and 20, 30 and 10 °C, respectively, compared to the non pretreated catalyst. Subsequently, it was observed in the reduced catalyst too that all three VOCs conversions increased with the lapse of reaction time at certain reaction temperatures (at 240 °C for benzene, at 190 °C for toluene and at 190 °C for *o*-xylene). The arrows in Fig. 7 show the points when the samples were withdrawn from the reactor for XPS and TEM analyses.

The BET surface areas, metal surface areas and Pd dispersions of the fresh pretreated catalyst, the pretreated catalyst used in this experiment (the arrow (c) in Fig. 7) and the used pretreated

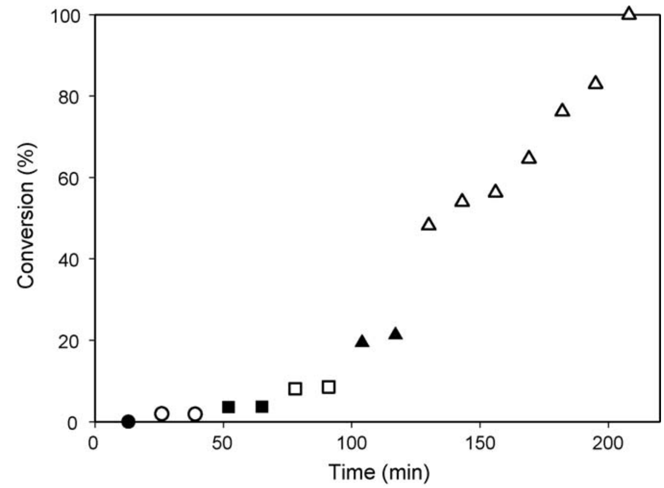

Fig. 8. Toluene conversion with time on stream over 1 wt% Pd/γ-Al_2O_3 catalyst pretreated with hydrogen. Reaction condition: catalyst weight = 0.2 g; toluene concentration = 1000 ppm; total flow rate = 100 cc min^{-1}. (●) 140 °C, (○) 150 °C, (■) 160 °C, (□) 170 °C, (▲) 180 °C, (△) 190 °C.

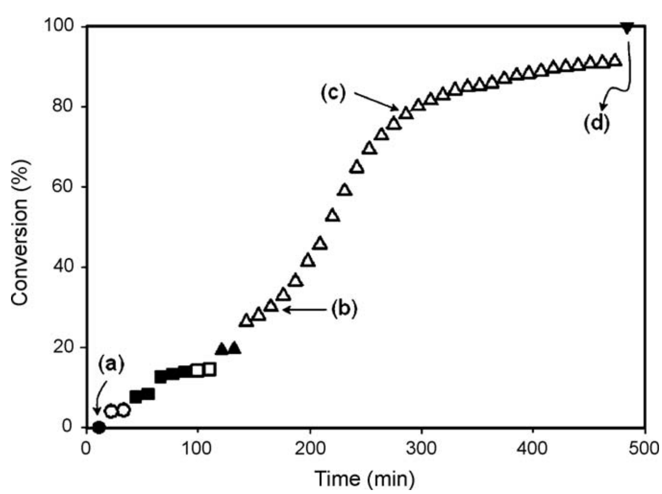

Fig. 7. Benzene conversion with time on stream over 1 wt% Pd/γ-Al_2O_3 catalyst pretreated with hydrogen. Reaction condition: catalyst weight = 0.2 g; toluene concentration = 1000 ppm; total flow rate = 100 cc min^{-1}. (●) 190 °C, (○) 200 °C, (■) 210 °C, (□) 220 °C, (▲) 230 °C, (△) 240 °C, (▼) 250 °C.

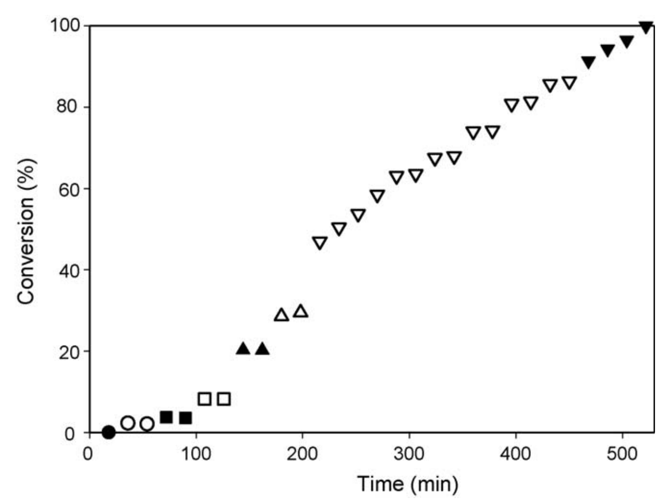

Fig. 9. Xylene conversion with time on stream over 1 wt% Pd/γ-Al_2O_3 catalyst pretreated with hydrogen. Reaction condition: catalyst weight = 0.2 g; toluene concentration = 1000 ppm; total flow rate = 100 cc min^{-1}. (●) 130 °C, (○) 140 °C, (■) 150 °C, (□) 160 °C, (▲) 170 °C, (△) 180 °C, (▼) 190 °C.

Table 2
Basic properties of 1 wt% Pd/γ-Al_2O_3 catalyst pretreated with hydrogen.

Catalyst	BET surface area ($m^2\,g^{-1}$)	Metal surface area ($m^2\,g^{-1}$)	Dispersion (%)
Fresh catalyst	150.2	2.68	60.2
Catalyst used in this experiment[a]	148.3	1.46	32.7
Used catalyst	147.1	1.30	29.0

[a] Catalyst after 140 min on stream at 240 °C in Fig. 7(c).

catalyst (the arrow (d) in Fig. 7) are summarized in Table 2. Their BET surface areas are similar within the experimental error, however, the metal surface area and its dispersion decreased considerably with the lapse of the reaction time also in the reduced samples.

Fig. 10 shows the Pd $3d_{5/2}$ XPS peaks and the binding energy values of the fresh catalyst, which was reduced by hydrogen prior to the catalytic activity (the arrow (a) in Fig. 7), the catalysts used in this experiment (the arrows (b) and (c) in Fig. 7) and the used catalyst (the arrow (d) in Fig. 7). As expected, the reduced sample showed the characteristics of metallic state (Pd^0) of which the binding energies (BEs) of Pd $3d_{5/2}$ is 334.5 eV, after hydrogen pretreatment. In the meantime, BEs of Pd $3d_{5/2}$ for the other three samples were found to be 334.5, 334.6 and 334.7 eV, respectively. Accordingly, the core level BEs of palladium (Pd $3d_{5/2}$) of all the catalysts fall under the category of those of the characteristics of metallic state (Pd^0) [18]. Also, the XPS results indicated that the oxidation state of palladium was insignificantly changed during the reaction, and subsequently, the increase of VOCs conversions with the lapse of reaction time at certain reaction temperatures (for benzene 240 °C; toluene 190 °C and *o*-xylene 190 °C) in Figs. 7–9, was independent of the oxidation state of palladium. However, the hydrogen treatment considerably improved the catalytic activity of 1 wt% Pd/γ-Al_2O_3 catalyst contributing to the formation of metallic Pd. Accordingly, it suggests that metallic palladium was more active than palladium oxide for VOCs total oxidation. These

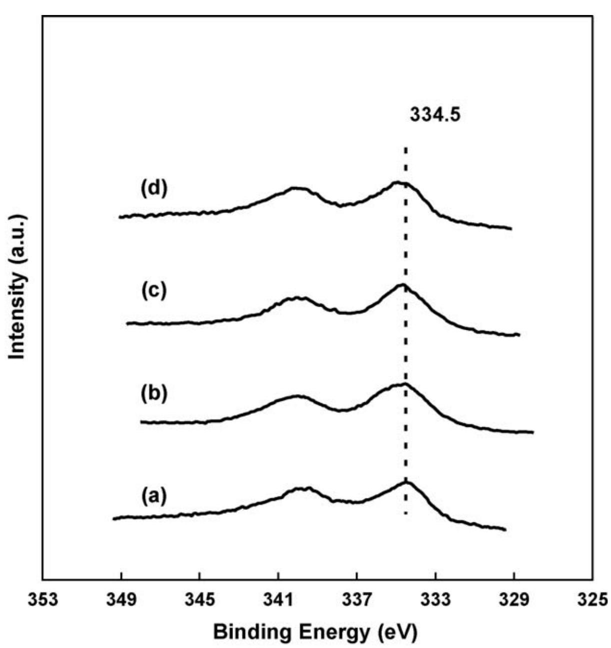

Fig. 10. XPS spectra of 1 wt% Pd/γ-Al_2O_3 catalyst: (a) the fresh catalyst, (b) the catalyst after 30 min on stream at 240 °C in Fig. 7, (c) the catalyst after 140 min on stream at 240 °C in Fig. 7, (d) the used catalyst in Fig. 7.

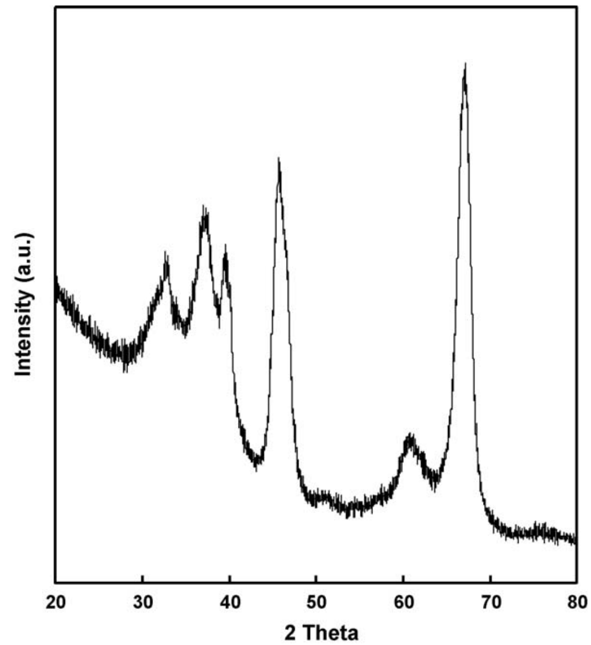

Fig. 11. XRD patterns of 1 wt% Pd/γ-Al_2O_3 catalyst treated with hydrogen.

results are also in good agreement with the previous works [18,20,21].

The XRD patterns of 1 wt% Pd/γ-Al_2O_3 catalyst pretreated with hydrogen are shown in Fig. 11. The diffraction peaks of γ-Al_2O_3 were observed in the reduced catalyst in a manner similar to the fresh catalyst. This indicates that Pd species were well dispersed on the support even after the pretreatment with hydrogen.

The changes in Pd particle size and morphology of 1 wt% Pd/γ-Al_2O_3 catalyst pretreated with hydrogen were explained by the TEM images, as shown in Fig. 12. The TEM image of the hydrogen pretreated sample is shown in Fig. 12(a). It was noticed that the hydrogen pretreatment increased the Pd particle sizes a little bit, and the observed particle sizes were in the range around 10–16 nm, which is comparatively bigger than that of 1 wt% Pd/γ-Al_2O_3 catalyst. The TEM images of the sample, which were collected during the oxidation and after the completion of the benzene oxidation, are shown in Fig. 12(b)–(d) (the same as the arrows (b)–(d) in Fig. 7). Fig. 12(b) represents the TEM image of the catalyst, which was sampled after 30 min lapsed at the reaction temperature of 240 °C. At this point the particle sizes insignificantly changed compared to those of the hydrogen pretreated catalyst. The TEM images of the catalysts (collected at 140 min) and the used catalyst (Fig. 12(c) and (d)) illustrated that Pd particle sizes gradually increased with the lapse of the reaction time to approximately 20–40 nm. It was also observed in the hydrogen pretreated catalyst that such an increase of the Pd particle sizes of the catalyst resulted in an increasing catalytic activity. These results reconfirmed that the VOC conversions are highly dependent on the growth of Pd particles in the catalyst. Moreover, the growth of Pd particle with the lapse of the reaction time could be well matched with the decreases of metal surface area and Pd dispersion (Table 2) at the reduced 1 wt% Pd/γ-Al_2O_3 catalyst too.

Finally, the results of Sections 3.1 and 3.2 suggest that both the oxidation state and the particle size of Pd had a great effect on the catalytic activity, and in the case of the catalyst consisting of the same oxidation state (PdO/Pd^{2+} or Pd^0), the particle sizes possibly play a more important role in the catalytic activity.

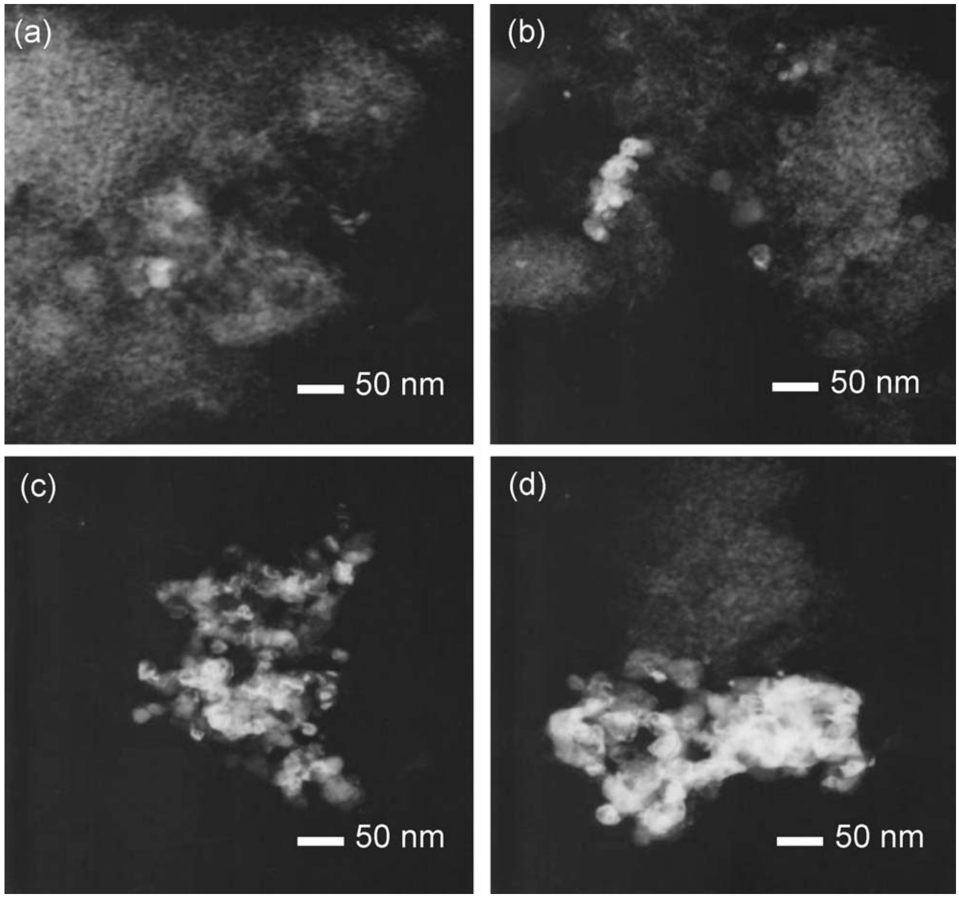

Fig. 12. TEM photographs of 1 wt% Pd/γ-Al_2O_3 catalyst: (a) the fresh catalyst, (b) the catalyst after 30 min on stream at 240 °C in Fig. 7, (c) the catalyst after 140 min on stream at 240 °C in Fig. 7, (d) the used catalyst in Fig. 7.

4. Conclusion

Catalytic oxidations of VOCs (benzene, toluene and *o*-xylene) were carried out over 1 wt% Pd/γ-Al_2O_3 catalyst and hydrogen pretreated 1 wt% Pd/γ-Al_2O_3. The experimental results revealed that the VOCs conversion significantly increased with the lapse of reaction time at certain reaction temperatures (without hydrogen pretreatment: at 270 °C for benzene, at 220 °C for toluene and at 200 °C for *o*-xylene, with hydrogen pretreatment: at 240 °C for benzene, at 190 °C for toluene and at 190 °C for *o*-xylene). The hydrogen pretreatment of the catalyst led the conversion curves for the total oxidation of VOCs to shift to lower temperature. The XPS results indicate that all the catalysts without hydrogen pretreatment (the fresh catalyst, the catalysts used in this experiment, and the used catalyst) showed the characteristics of oxidized state (PdO/Pd^{2+}), and the catalysts with hydrogen pretreatment showed that of metallic state (Pd^0). The TEM results showed that Pd particle sizes increased with the lapse of reaction time at certain reaction temperatures. The increase in VOCs conversion with the lapse of reaction time at certain reaction temperatures was highly dependent on the growth of Pd particles on the catalyst. In addition, both the oxidation state and the particle size of Pd had a great effect on the catalytic activity, and in the case of the catalyst consisting of the same oxidation state (PdO/Pd^{2+} or Pd^0), the particle sizes possibly play a more important role in the catalytic activity. The activity of 1 wt% Pd/γ-Al_2O_3 catalyst with respect to the VOC molecule was observed to follow sequence: *o*-xylene > toluene > benzene, indicating the ionization potentials of methyl derivatives of reactants had an effect on the catalytic activity.

Acknowledgement

This subject is supported by Ministry of Environment of the Republic of Korea as "The Eco-technopia 21 project".

References

[1] M. Lamallem, H. El Ayadi, C. Gennequin, R. Cousin, S. Siffert, F. Aïssi, A. Aboukaïs, Catal. Today 137 (2008) 367–372.
[2] E.N. Ruddy, L.A. Carroll, Chem. Eng. Prog. 89 (1993) 28–35.
[3] I. Khan, A.K. Ghoshal, J. Loss Prev. Proc. 13 (2000) 527–545.
[4] K. Everaert, J. Baeyens, J. Hazard. Mater. B: Environ. 109 (2004) 113–139.
[5] M. Guillemot, J. Mijoin, S. Mignard, P. Magnoux, Appl. Catal. B: Environ. 75 (2007) 249–255.
[6] T. Garcia, B. Solsona, D.M. Murphy, K.L. Antcliff, S.H. Taylor, J. Catal. 229 (2005) 1–11.
[7] J. Tsou, P. Magnoux, M. Guisnet, J.J.M. Órfão, J.L. Figueiredo, Appl. Catal. B: Environ. 57 (2005) 117–123.
[8] B. Grbic, N. Radic, A. Terlecki-Baricevic, Appl. Catal. B: Environ. 50 (2004) 161–166.
[9] E.M. Cordi, P.J. O'Neill, J.L. Falconer, Appl. Catal. B: Environ. 14 (1997) 23–36.
[10] S.C. Kim, J. Hazard. Mater. B91 (2002) 285–299.
[11] C.H. Wang, S.S. Lin, C.L. Chen, H.S. Weng, Chemosphere 64 (2006) 503–509.
[12] Y. Li, X. Zhang, H. He, Y. Yu, T. Yuan, Z. Tian, J. Wang, Y. Li, Appl. Catal. B: Environ. 89 (2009) 659–664.
[13] B. Gric, N. Radic, Z. Arsenijevic, R. Garic-Grulovic, Z. Grbavcic, Appl. Catal. B 90 (2009) 478–484.
[14] E.M. Cordi, J.L. Falconer, J. Catal. 162 (1996) 104–117.
[15] R.S.G. Ferreira, P.G.P. de Oliveira, F.B. Noronha, Appl. Catal. B: Environ. 50 (2004) 243–249.
[16] T. Garcia, B. Solsona, D. Cazorla-Amoros, A. Linares-Solano, S.H. Taylor, Appl. Catal. B: Environ. 62 (2006) 66–76.
[17] A.F. Pérez-Cadenas, S. Morales-Torres, F. Kapteijn, F.J. Maldonado-Hódar, F. Carrasco-Marín, C. Moreno-Castilla, J.A. Moulijn, Appl. Catal. B: Environ. 77 (2008) 272–277.
[18] S.K. Ihm, Y.D. Jun, D.C. Kim, K.E. Jeong, Catal. Today 93–95 (2004) 149–154.
[19] P. Dege, L. Pinard, P. Magnoux, M. Guisnet, Appl. Catal. B: Environ. 27 (2000) 17–26.

[20] W.G. Shim, J.W. Lee, S.C. Kim, Appl. Catal B: Environ. 84 (2008) 133–141.
[21] S. Huang, C. Zhang, H. He, Catal. Today 139 (2008) 15–23.
[22] Y. Yazawa, H. Yoshida, N. Takgi, S. Komai, A. Satsuma, T. Hattori, Appl. Catal. B19 (1996) 261–266.
[23] R. Burch, P.K. Loader, F.J. Urbano, Catal. Today 27 (1996) 243–248.
[24] K. Muto, N. Katada, M. Niwa, Appl. Catal. 134 (1996) 203–215.
[25] T.R. Baldwin, R. Burch, Appl. Catal. 66 (1990) 337–358.
[26] Y. Yazawa, H. Yoshida, N. Takagi, S. Komai, A. Satsuma, T. Hattori, J. Catal. 187 (1999) 15–23.
[27] P. Briot, M. Primet, Appl. Catal. 68 (1991) 301.
[28] C.A. Muller, M. Maciejewski, R.A. Koeppel, A. Maiker, J. Catal. 166 (1997) 36–43.
[29] P. Papaefthimiou, T. Ioannides, X.E. Verykios, Appl. Catal. B: Environ. 13 (1997) 175–184.
[30] R.J. Farrauto, M.C. Hobson, T. Kennelly, E.M. Waterman, Appl. Catal. A 81 (1992) 227–237.
[31] M. Lyubovsky, L. Pfefferle, Appl. Catal. 173 (1998) 107–119.
[32] O. Demoulin, G. Rupprechter, I. Seunier, B. Le Clef, M. Navez, P. Ruiz, J. Phys. Chem. B 109 (2005) 20454–20462.
[33] A. Baylet, S. Royer, P. Marecot, J.M. Tatibouet, D. Duprez, Appl. Catal. B: Environ. 81 (2008) 88–96.